Mechanism of the Reaction of Different Phosphates with the Iron(II)iron(III) form of Purple Acid Phosphatase from Porcine Uteri (Uteroferrin)†

Manuel A. S. Aquino, Joo-Sang Lim and A. Geoffrey Sykes*
Department of Chemistry, The University of Newcastle, Newcastle upon Tyne NE1 7RU, UK

Reactions of different phosphates (represented here as PO_4), including $H_2PO_4^-$ (as prototype), phenylphosphate (and the *p*-nitro derivative), pyrophosphate, tripolyphosphate, and adenosine 5'-triphosphate (ATP), with the $Fe^{II}Fe^{III}$ form of purple acid phosphatase (PAP_r) from porcine uteri (uteroferrin) have been studied by monitoring absorbance changes for the iron(III) chromophore at 620 nm. Stopped-flow rate constants are independent of total [PO_4] (10–50 mM), and decrease with increasing pH (2.5–6.5). At the lower pH a mechanism of rapid PO_4 binding to the Fe^{II}, followed by rate-controlling [PO_4]-independent bridging to the Fe^{III} with displacement of a co-ordinated H_2O, is proposed. Further information comes from experiments on the hydrolysis activity of PAP, monitored by the release of α-naphthol (323 nm) from α-naphthyl phosphate, which maximises at pH 4.9. The full mechanism requires participation of Fe^{III}–OH, which substitutes into the phosphate moiety thus bringing about hydrolysis. The concentration of the latter peaks at pH 4.9, and possible reasons for the decrease in activity at pH >4.9 are given. Rate constants at maximum activity are of magnitude $\approx 0.5\ s^{-1}$ only, with no very strong discrimination between the reagents used. Equilibration steps in which the phosphate can if necessary be recycled to bring about hydrolysis are proposed. For the pH range studied the final product has a bridging HPO_4^{2-} ligand. Trimethyl phosphate with only one oxo group does not appear to react at the Fe^{III}, but inhibits reaction with $H_2PO_4^-$ possibly by co-ordinating to the Fe^{II}. Reaction with the sterically bulky cation $[Co(NH_3)_5(HPO_4)]^+$ is much slower, $k = 1.6 \times 10^{-4}\ s^{-1}$. The HPO_4^--bridged $Fe^{II}Fe^{III}$ form is more responsive to air oxidation to $Fe^{III}Fe^{III}$ consistent with the decrease in reduction potential from 367 and 183 mV. Rate constants are independent of [$H_2PO_4^-$] and pH.

The purple acid phosphatases (PAPs) are iron-containing glycoproteins which can be isolated from animal and plant species. The most widely studied PAPs are those obtained from mammalian sources, for example the allantoic fluids of the uteri of a pregnant pig (uteroferrin), and from bovine spleens.[1–5] Both these proteins, $M_r \approx 35\,000$, have a single polypeptide chain (318 amino acids),[6] and a binuclear iron site. The active form of the protein is in the $Fe^{II}Fe^{III}$ state, which catalyses the hydrolysis of phosphate esters, equation (1). Whether this is

$$O_3P(OR)^{2-} + H_2O \longrightarrow HPO_4^{2-} + ROH \quad (1)$$

their exclusive role remains to be established, since there is evidence that PAP can for example transfer its Fe to transferrin.[7] The presence of relatively large amounts of the protein in the uterus also suggests that there may be some alternative role.

There is a 90% sequence homology between uteroferrin and beef-spleen PAP,[6,8] and Mössbauer,[9,10] EPR[4,11] and resonance-Raman[12,13] studies have indicated similarities in the active sites of the two proteins. Plant PAPs of higher M_r having different metal components, kidney bean (Fe/Zn),[14] and sweet potatoes (2Fe or 2Mn),[15,16] have also been reported. A crystal structure is in progress from the Fe/Zn kidney bean protein.[17]

The mammalian $Fe^{II}Fe^{III}$ protein (PAP_r) has a characteristic pink colour with a peak at 515 nm ($\varepsilon = 4000\ M^{-1}\ cm^{-1}$), and the inactive $Fe^{III}Fe^{III}$ form (PAP_o) a purple colour with peak at 550 nm ($\varepsilon = 4000\ M^{-1}\ cm^{-1}$).[18,19] The absorption arises in large part from the tyrosine→Fe^{III} ligand-to-metal charge transfer (l.m.c.t.) at the (normally) redox-inactive iron(III) centre.[4,20] The UV/VIS spectrum is therefore sensitive to co-ordination at the Fe^{III} and not the Fe^{II}. In addition the co-ordination of one histidine to each Fe, and likelihood of carboxylate co-ordination by Asp or Glu has been suggested from extended X-ray absorption fine structure (EXAFS),[21] NMR[22–25] and EPR studies.[26,27] Magnetic susceptibility measurements[4,13,28,29] have indicated $-J \leqslant 40$ and $\leqslant 150\ cm^{-1}$ for the $Fe^{III}Fe^{III}$ form consistent with antiferromagnetic coupling. Upon reduction to $Fe^{II}Fe^{III}$ the $-J$ values drop to between 5 and 11 cm^{-1}. Recent analysis of iron K-edge EXAFS data[30] for the $Fe^{III}Fe^{III}$ protein suggest a μ-hydroxo or alkoxy bridge supported by a μ-carboxylato group, rather than a μ-oxo bridge, in agreement with $-J$ values of $\leqslant 40\ cm^{-1}$. The same paper provides evidence for a μ-hydroxo (or possibly μ-alkoxo) structure for the $Fe^{II}Fe^{III}$ protein. The diiron site has similarities to that in ribonucleotide reductase and methane monooxygenase.[30] There are two aspects of the structure which require emphasis in the context of the present studies. First the existence of co-ordinated H_2O groups to each Fe has been demonstrated by ESEEM,[31] and electrochemical studies[32] on PAP_r. Secondly the Fe–Fe and Fe–P distances determined from EXAFS on $PAP_o{\cdot}PO_4$ are consistent with a bridging phosphate.[30] The most recently proposed structures[30] for PAP_r and $PAP_o{\cdot}PO_4$ are as indicated in Fig. 1, see also ref. 1. Although not precise these give a strong indication as to the nature of the binuclear iron site from studies using physical techniques.

Also relevant are the recent results obtained from the reaction of labelled adenosine 5'-triphosphate (ATP) with PAP_r, which in a very elegant way have distinguished between three possible mechanisms. This work has demonstrated that there is transfer of phosphate to an H_2O position on the PAP with overall inversion at the phosphate.[33]

Reactions of other oxy-anions with the active $Fe^{II}Fe^{III}$ form of the protein have been reported.[18,23–26] A number of oxy-anions have been shown to inhibit the hydrolysis of phosphate-

† *Non-SI unit employed:* M = mol dm^{-3}.

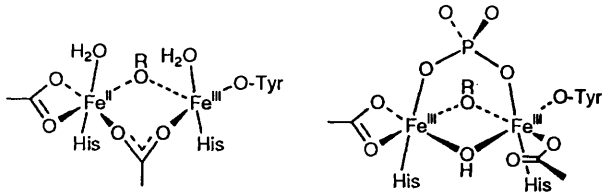

Fig. 1 Recently proposed structures of the diiron sites in active $Fe^{II}Fe^{III}$ PAP_r, and in the $Fe^{III}Fe^{III}$ adduct $PAP_o{\cdot}PO_4$, from ref. 30 [OR represents an hydroxo (or alkoxo)bridge]

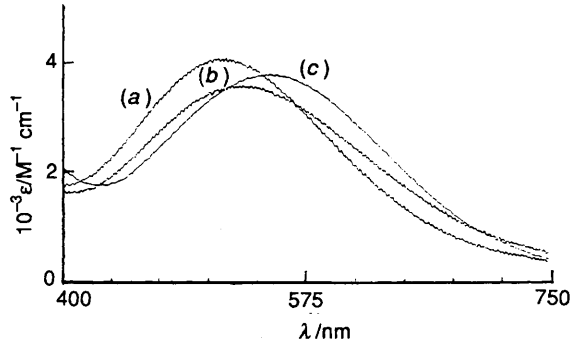

Fig. 2 Visible spectra of (*a*) a 30 μM solution of the $Fe^{II}Fe^{III}$ form of PAP (uteroferrin), (*b*) with the addition of 8 mM $H_2PO_4^-$ and (*c*) the phosphate-bound $Fe^{III}Fe^{III}$ PAP_o product obtained on air oxidation, all at pH 4.9, I = 0.100 M (NaCl)

containing substrates. For example, arsenate as well as phosphate can act as a weak inhibitor (K_i = 2–15 mM) and molybdate and tungstate as stronger inhibitors (K_i = 2 and 1 μM respectively) in the hydrolysis of *p*-nitrophenyl phosphate.[37] An essential part of the reaction steps proposed is the replacement of H_2O ligands, one to each metal.[34]

The addition of $H_2PO_4^-$ to the $Fe^{II}Fe^{III}$ protein (PAP_r) leads to rapid formation of a phosphato product, which has a very broad EPR signal.[18] Kinetic studies on this reaction reported in an earlier communication [38] have now been extended to include consideration of phenyl phosphate and its *p*-nitro derivative, pyrophosphate ($P_2O_7^{4-}$), tripolyphosphate ($P_3O_{10}^{5-}$), ATP, α-naphthyl phosphate, trimethyl phosphate and $[Co(NH_3)_5(HPO_4)]^{2+}$, all of which undergo hydrolysis. As a result a mechanism for the reaction of these and related esters with PAP_r is proposed.

The abbreviation PO_4 is used to denote the different phosphate derivatives.

Experimental

Isolation of PAP (Uteroferrin).—Uteroferrin was obtained from the allantoic fluid of a sow at mid-pregnancy, and purified according to a literature procedure.[18] The product isolated consists of about equal amounts of active and inactive PAP_r and PAP_o, the latter with phosphate bound. The PAP_o protein was reduced to the $Fe^{II}Fe^{III}$ state with 0.1 M ascorbate and 6 mM ammonium iron(II) sulfate in 0.05 M acetate buffer at pH 5.0. This was followed by desalting on a Sephadex G25 column and buffer exchange using an Amicon filter with PM10 membrane. Yields of protein were 400–600 mg. As required the absorbance ratio A_{280}/A_{515} for pure PAP_r gave a value of less than 15:1. The purified protein was dialysed against 40 mM acetate buffer, pH 4.9, and concentrated using an Amicon filter. The concentration of PAP_r was determined from the absorbance peak at 515 nm using a molar absorption coefficient of 4000 M^{-1} cm^{-1}, Fig. 2.[39] The protein could be stored indefinitely at −80 °C under air. A small amount (≈25 mg) of a high M_r heterodimer was also obtained.

Other Reagents.—The following reagents were used as supplied: potassium dihydrogen(ortho)phosphate, KH_2PO_4 (BDH, AnalaR); disodium phenyl phosphate, $Na_2C_6H_5PO_4{\cdot}2H_2O$ (Aldrich); tetrasodium pyrophosphate (diphosphate), $Na_4P_2O_7{\cdot}10H_2O$ (BDH, AnalaR); pentasodium tripolyphosphate, $Na_5P_3O_{10}{\cdot}6H_2O$ (Sigma); disodium adenosine 5′-triphosphate, ATP; trimethyl phosphate, $OP(OMe)_3$ (both Aldrich); and disodium α-naphthyl phosphate, $Na_2C_{10}H_7PO_4{\cdot}H_2O$ (Sigma) and *p*-nitrophenylphosphate (Aldrich). Stock solutions of the various phosphates were made up with appropriate buffer. The complex $[Co(NH_3)_5(PO_4)]{\cdot}2H_2O$ was prepared by an established procedure, and characterised by the UV/VIS spectrum of $[Co(NH_3)_5(HPO_4)]^+$ at pH 5, λ/nm (ε/M^{-1} cm^{-1}) 359 (61.6) and 521 (77.8).[40]

Buffers.—Different buffers (40 mM) were used for the pH range investigated as follows: glycine–HCl, pH 2.5–3.2; acetate–acetic acid, pH 3.2–5.6; 2-morpholinoethanesulfonic acid (mes)–NaOH, pH 5.8–6.5; and [bis(2-hydroxyethyl)amino]-tris(hydroxymethyl)methane (bis–tris)/HCl, pH 5.8–7.2, all from Sigma. All buffers were prepared using water which had been singly distilled and then deionised. Buffer solutions were prepared with the addition of 0.10 mM ethylenediaminetetra-acetate to complex any adventitious Fe.

Reaction Products.—From the spectroscopic and chemical properties of the final (stopped-flow) products as determined in this and other work it can be concluded that the phosphate is co-ordinated as μ-HPO_4^{2-} for the pH range explored here. As a part of the mechanism proposed in this study, hydrolysis of the different phosphates to give the μ-HPO_4^{2-} product does not always occur on the first bridge closure, and re-equilibration involving recycling of the unhydrolysed phosphate reactant is necessary.

Kinetic Studies.—Studies on the reactions of different phosphates with PAP_r do not require air-free conditions. Ionic strengths were adjusted to 0.100 ± 0.001 M with sodium chloride, and the temperature was 25.0 ± 0.1 °C. The pH of solutions was checked before and after each run. Spectrophotometric changes for $H_2PO_4^-$ complexing gave a shift from 515 nm for PAP_r to 535–560 nm for the $PAP_r{\cdot}PO_4$ form (which is pH dependent). Slower absorbance changes to a 550 nm peak occur subsequently, consistent with air oxidation to the $PAP_o{\cdot}PO_4$ form, Fig. 2. The kinetics of the formation of $PAP_r{\cdot}PO_4$ was monitored at 620 nm (absorbance increase), or in a number of check runs at 480 nm (absorbance decrease), using a Dionex D-110 stopped-flow spectrophotometer. Protein concentrations were in the range (1.5–3.0) × 10^{-5} M with the different phosphate substrates in >40-fold excess. The amplitude of the absorbance changes depends on the phosphate concentration and the reactions are therefore equilibration processes. Absorbance against time changes were satisfactorily fitted by a uniphasic first-order process, rate constants k_{obs}, using an OLIS software package.[41] The fits were equally satisfactory with *e.g.* $H_2PO_4^-$ and ATP, where in the latter case recycling to bring about complete hydrolysis may be required (see later). Absorbance changes are often small restricting the range of possible studies.

The slower phosphate-induced air oxidation of PAP_r was monitored by conventional spectrophotometry (Shimadzu UV2101-PC). Prior to mixing the protein was dialysed against air-saturated buffer, and air-saturated phosphate was then added. The oxidation was monitored at 600–625 nm. The formation constant K for phosphate binding to PAP_r has been determined previously from inhibition studies, and values ranging from 83 to 313 M^{-1} are apparent at pH ≈5.[18,39] Concentrations of $H_2PO_4^-$ ≥9 mM were required to maintain a sufficiently high $PAP_r{\cdot}PO_4$ level. First-order rate constants k_{ox} were obtained by fitting of absorbance against time data using a non-linear least-squares program.

Procedure for Measuring PAP_r *Activity.*—Phosphatase activity at 25 °C was measured by treating α-naphthyl phosphate (10 mM) with PAP_r (0.023 μM) and recording the absorbance increase due to α-naphthol release at the 323 nm peak ($\varepsilon = 2040\ M^{-1}\ cm^{-1}$). The initial slope of a plot of α-naphthol released against time gave the activity in nmol min^{-1}. Runs were carried out at pH 3.2–6.5 using acetate and bis-tris buffers, $I = 0.100$ M(NaCl). In previous work unit enzyme activity was defined as the amount of enzyme catalysing the hydrolysis of 1 μmol of α-naphthyl phosphate per min at 20 °C.[34]

Results

Rate Law Dependencies on $[PO_4]$.—At pH 4.6 first-order rate constants k_{obs} were found to be independent of $[PO_4]$ for $H_2PO_4^-$, phenyl phosphate, pyrophosphate, tripolyphosphate and ATP. No reaction was observed with trimethyl phosphate. Amounts of $[PO_4]$ were varied over the range 10–50 mM, Fig. 3. The independence of k_{obs} on $[PO_4]$ was also confirmed at pH 5.3. At pH 4.6 values of k_{obs} for the different phosphates vary from 1.2 to 2.3 s^{-1}. Rate constants in the case of phosphate and phenyl phosphate were shown to be independent of acetate buffer (25–55 mM). Reactions at pH 4.6 with $[PO_4] < 5$ mM could not be monitored satisfactorily due to small absorbance changes for the overall process (2). In the case of $H_2PO_4^-$ (5

$$PAP_r + PO_4 \overset{K}{\rightleftharpoons} PAP_r{\cdot}PO_4 \qquad (2)$$

mM), with $K = 83\ M^{-1}$ at pH 5.0,[18] only ≈30% of the protein is present as $PAP_r{\cdot}PO_4$. Similar observations apply for the other phosphate derivatives. As a result spectrophotometric changes are more difficult to monitor. At $[PO_4] > 60$ mM protein denaturation is observed.

pH *Dependence.*—First-order rate constants k_{obs}, Table 1, for the binding of $H_2PO_4^-$, phenyl phosphate, pyrophosphate, tripolyphosphate, and ATP are dependent on pH in the range 2.6–6.5, Figs. 4 and 5. Possible effects of $[H^+]$ are from free and monodentate phosphate forms as well as the aqua ligands and protein amino-acid residues. In the case of $H_2PO_4^-$ only a single pK_a is observed, Fig. 4. In all other cases, Figs. 4 and 5, two pK_a values (pK_{1a} and pK_{2a}) are noted, and rate constants k_1, k_2 and k_3 can be defined for the reactions of different protonated/deprotonated forms. The reaction mechanism is illustrated in Scheme 1 for $H_2PO_4^-$, although for this particular

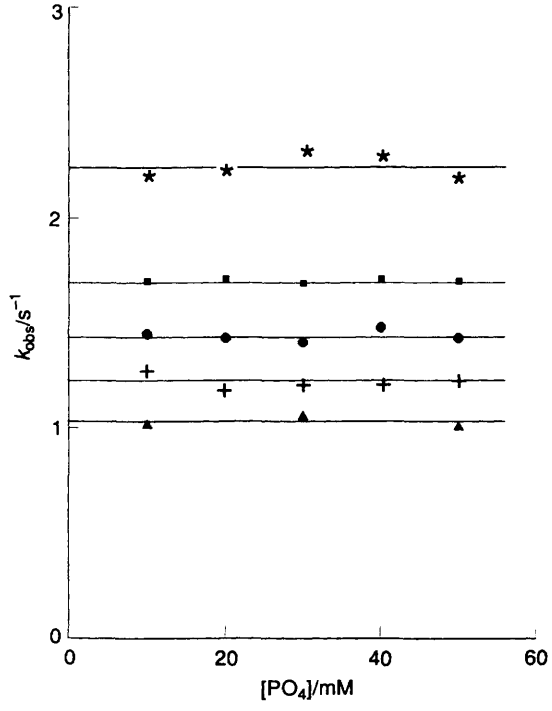

Fig. 3 The invariance of first-order rate constants k_{obs} (25 °C) on phosphate concentration for the reaction of the active $Fe^{II}Fe^{III}$ form of PAP_r (uteroferrin) with different phosphates $H_2PO_4^-$ (■), phenyl phosphate (+), pyrophosphate (★), tripolyphosphate (●) and ATP (▲) at pH 4.6, $I = 0.100$ M (NaCl)

Table 1 The variation of rate constants (25 °C) with pH for the reactions of different phosphates with active $Fe^{II}Fe^{III}$ PAP (uteroferrin), $I = 0.100$ M (NaCl)

(*a*) $H_2PO_4^-$

pH	2.73	3.01	3.48	3.70	4.01	4.16	4.32	4.61	4.81
k_{obs}/s^{-1}	6.8	6.4	5.3	4.7	3.6	2.83	2.26	1.70	1.24
pH	5.02	5.30	5.58	6.00	6.50				
k_{obs}/s^{-1}	1.24	0.91	0.56	0.50	0.42				

(*b*) Phenyl phosphate

pH	2.61	2.98	3.23	3.51	3.71	3.98	4.30	4.64
k_{obs}/s^{-1}	7.2	6.3	5.4	3.9	3.0	2.08	1.51	1.09
pH	4.78	4.97	5.12	5.25	5.45	5.68	5.93	6.26
k_{obs}/s^{-1}	0.89	0.80	0.77	0.65	0.40	0.32	0.21	0.16

(*c*) Pyrophosphate

pH	3.15	3.30	3.60	3.70	3.85	3.97	4.20	4.60
k_{obs}/s^{-1}	3.8	3.7	3.4	3.2	2.68	2.53	2.30	2.20
pH	5.02	5.30	5.43	5.54	6.01			
k_{obs}/s^{-1}	2.14	1.72	1.08	0.76	0.67			

(*d*) Tripolyphosphate

pH	3.00	3.15	3.30	3.55	3.78	3.87	4.11	4.46
k_{obs}/s^{-1}	2.69	2.65	2.55	2.46	2.08	1.70	1.61	1.50
pH	4.79	4.91	5.12	5.41	6.02	6.42		
k_{obs}/s^{-1}	1.45	1.24	0.79	0.52	0.41	0.35		

(*e*) ATP

pH	3.03	3.37	3.65	3.78	4.04	4.25	4.55	5.11
k_{obs}/s^{-1}	3.5	3.2	2.57	1.75	1.55	1.32	1.02	0.96
pH	5.65	5.92						
k_{obs}/s^{-1}	0.85	0.84						

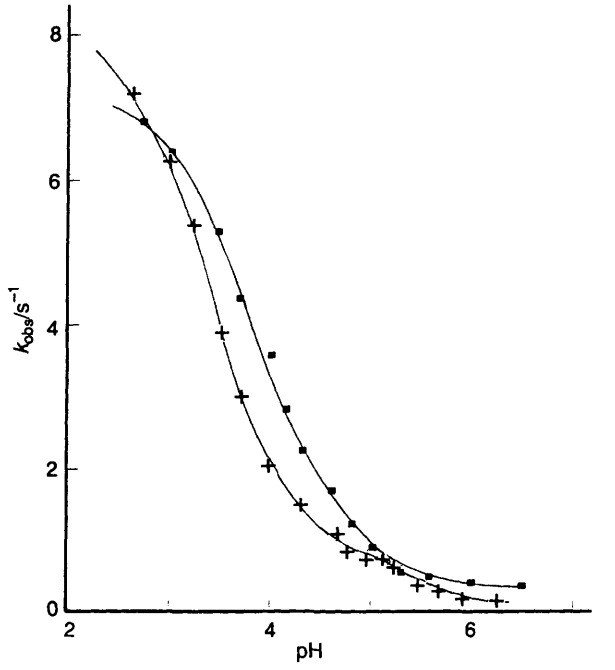

Fig. 4 Variation of first-order rate constants k_{obs} (25 °C) with pH for the reaction of the active $Fe^{II}Fe^{III}$ form PAP_r (uteroferrin), with $H_2PO_4^-$ (■) and phenyl phosphate (+), $I = 0.100$ M (NaCl)

Table 2 Summary of data obtained for the reactions (25 °C) of $H_2PO_4^-$, phenyl phosphate, pyrophosphate, tripolyphosphate and ATP with active $Fe^{II}Fe^{III}$ PAP (uteroferrin) at pH 2.6–6.5, I = 0.10 M (NaCl)

	$H_2PO_4^-$	Phenylphosphate	Pyrophosphate	Tripolyphosphate	ATP
pK_{a1}	≈3.9	≈3.4	≈3.6	≈3.7	≈3.7
pK_{a2}	—	5.2(2)	5.3(4)	5.0(2)	≈4.2
k_1/s^{-1}	7.1(1)	8.4(2)	4.7(4)	3.1(2)	≈3.8
k_2/s^{-1}	—	1.0(3)	2.3(4)	1.5(2)	≈1.5
k_3/s^{-1}	0.38(6)	< 0.1(1)	0.1(6)	0.2(1)	≈0.8

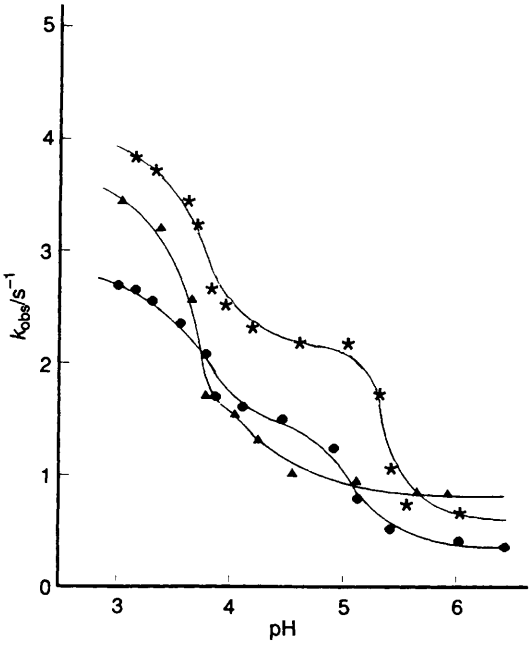

Fig. 5 Variation of first-order rate constants k_{obs} (25 °C) with pH for the reaction of active $Fe^{II}Fe^{III}$ PAP_r (uteroferrin) with pyrophosphate (★), tripolyphosphate (●) and ATP (▲), I = 0.100 M (NaCl)

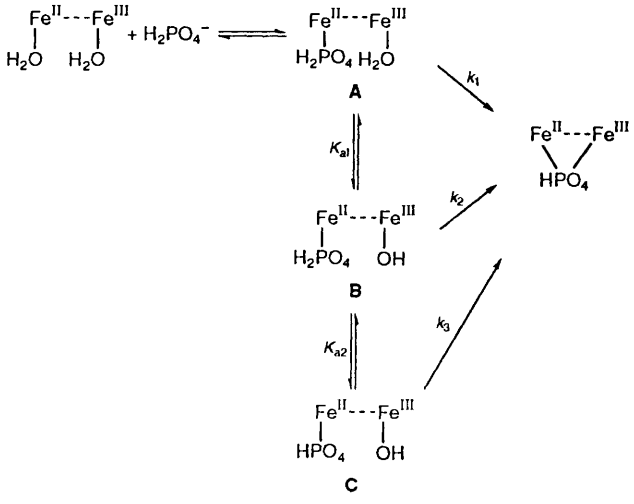

Scheme 1 Mechanism for the reaction of $Fe^{II}Fe^{III}$ PAP_r (uteroferrin) with phosphate ($H_2PO_4^-$) defining rate constants (k) and acid dissociation constants (K_a). Step k_3 is not detected for this particular reactant at pH < 6.5 but is observed in reactions with other phosphates, see Table 3

reactant and the conditions of pH employed pK_{2a} (and k_3) do not in fact contribute. From Scheme 1 the rate equation (3), can be derived by first of all equating the rate expressions

$$k_{obs} = k_1 + \frac{(k_3 - k_1)K_{1a}K_{2a} + (k_2 - k_1)K_{1a}[H^+]}{[H^+]^2 + K_{1a}[H^+] + K_{1a}K_{2a}} \quad (3)$$

$k_{obs}([A] + [B] + [C])$ and $k_1[A] + k_2[B] + k_3[C]$. Substituting in for [A] and [B] using expressions for K_{1a} and K_{2a} gives equation (4) which can be rearranged to give (3). From fits to (3), values of K_{1a}, K_{2a}, k_1, k_2 and k_3 are obtained, Table 2. From a comparison of pK_a values, Table 2, with those

$$k_{obs}\left(\frac{[H^+]^2}{K_{1a}K_{2a}} + \frac{[H^+]}{K_{2a}} + 1\right) = \frac{k_1[H^+]^2}{K_{1a}K_{2a}} + \frac{k_2[H^+]}{K_{2a}} + k_3 \quad (4)$$

for the unco-ordinated phosphates, Table 3, it is possible to assign these to monodentate phosphate derivatives.[46] Also since k_{obs} arises from an equilibration process it can be expressed as the sum of forward and back rate constants, in the general case as $k_f + k_b$.

Absorbance changes for the reaction of *p*-nitrophenyl phosphate (10.5 mM) with PAP_r (1.42×10^{-5} M) at 620 nm give rate constants 5.6, 4.5 and 2.4 s^{-1} at pH 3.18, 3.54 and 3.89 respectively, which are very similar to those obtained for phenyl phosphate. It was not possible to measure rate constants for the corresponding α-naphthyl phosphate reaction because at the concentrations required for such studies precipitation of α-naphthol occurs.

Determination of Formation Constants.—The overall formation constant K, equation (2), can be expressed as in (5), where

$$\frac{1}{(A_0 - A_{obs})} = \frac{K}{[PO_4][A_0 - A_\infty)} + \frac{1}{(A_0 - A_\infty)} \quad (5)$$

A_0 and A_∞ are the absorbances of PAP_r and $PAP_r{\cdot}PO_4$ respectively, and A_{obs} is the experimental value for a particular $[PO_4]$. Plots of $(A_0 - A_{obs})^{-1}$ against $[PO_4]^{-1}$ are shown in Fig. 6 for $H_2PO_4^-$ (pH 5.0) which gives $K = 112 \pm 7$ M^{-1}, and for ATP (pH 4.6) $K = 28 \pm 7$ M^{-1}.

Monitoring of Activity.—In the case of α-naphthyl phosphate it was possible to monitor the release of the α-naphthol product from absorbance changes at 323 nm. Fig. 7 is the resultant activity plot.

Inhibition Studies.—No absorbance changes are observed on addition of trimethylphosphate (55 mM) to PAP_r (1.9×10^{-5} M). However the reaction of $H_2PO_4^-$ (11 mM) with PAP_r (1.9×10^{-5} M) is inhibited by addition of $OP(OMe)_3$ (55 mM), and no stopped-flow absorbance changes were observed at pH 5.0. This suggests attachment of $OP(OMe)_3$ to the Fe^{II} with resultant inhibition of the $H_2PO_4^-$ reaction.

Reaction of $[Co(NH_3)_5(HPO_4)]^+$ *with* PAP_r.—Whether PAP_r can similarly hydrolyse a co-ordinated cationic phosphato complex was of further interest. At pH 5.0 no absorbance changes were observed over 3 h for a solution of $[Co(NH_3)_5(HPO_4)]^+$ (1.7×10^{-4} M) with PAP_r (1.3×10^{-5} M). At higher concentrations, $[Co(NH_3)_5(HPO_4)]^+$

Table 3 Summary of literature acid dissociation pK_a values (25 °C) for H_3PO_4, phenylphosphate, pyrophosphate, tripolyphosphate and ATP, I = 0.100 M or as stated

	H_3PO_4[a]	Phenylphosphate[b]	Pyrophosphate[c]	Tripolyphosphate[d]	ATP[e]
pK_1	2.12	0.30	2.5	Small	
pK_2	6.7	5.63	2.7	2.2	
pK_3	12.7	—	6.0	2.6	
pK_4	—	—	8.3	5.6	4.26
pK_5	—	—	—	7.9	6.73

[a] At 25 °C, I = 0.10 M ($NaClO_4$).[42] [b] At 25 °C, I = 0.25 M ($NaClO_4$).[43] [c] At 25 °C, I = 0.10 M ($NaNO_3$).[44] [d] At 25 °C, I = 0.10 M ($NaNO_3$).[44] [e] At 25 °C, I = 0.10 M (KCl).[45]

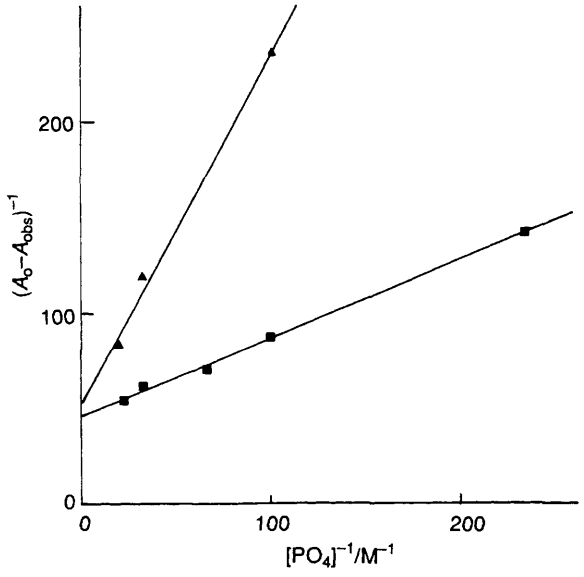

Fig. 6 Determination of the formation equilibrium constant (25 °C) for the reaction of PAP_r (uteroferrin) with $H_2PO_4^-$ (■, pH 5.0) and ATP (▲, pH 4.6), I = 0.100 M (NaCl)

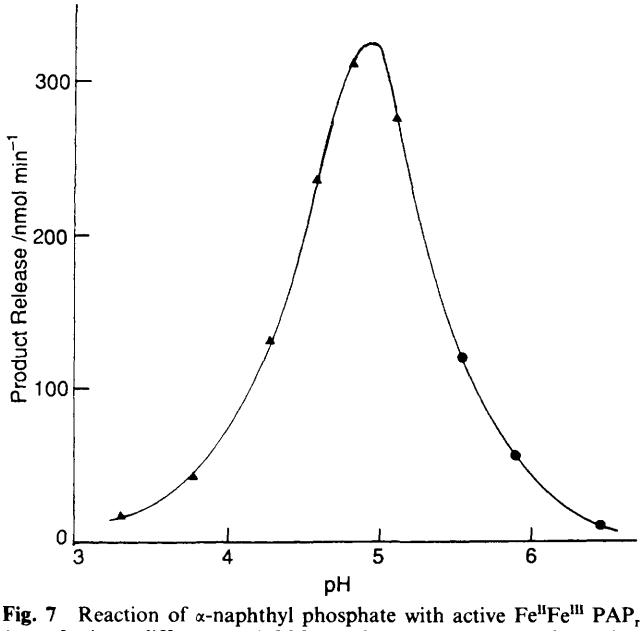

Fig. 7 Reaction of α-naphthyl phosphate with active $Fe^{II}Fe^{III}$ PAP_r (uteroferrin) at different pH (25 °C) monitored by α-naphthol formation at 323 nm, I = 0.100 M (NaCl). The product release indicated is an initial slope. Buffers: 40 mM acetate (▲) and bis-tris (●)

(1.0×10^{-3} M) and PAP_r (2.5×10^{-5} M), absorbance changes over 17 h gave a rate constant 1.6×10^{-4} s^{-1} in a strictly uniphasic process. Even at 60 °C aquation of the parent complex with release of phosphate is an order of magnitude slower than the reaction observed here.[40b] The absorbance peak shifts from 521 to 526 nm consistent with phosphate complexing, and isosbestic points were observed at 424 and 531 nm.

Phosphate-induced Oxidation of PAP_r *by* O_2.—The adduct PAP_r·PO_4 shows an increased sensitivity to air oxidation as compared to PAP_r, to give the catalytically inactive PAP_o·PO_4 product, Fig. 2. First-order kinetics observed for the formation of PAP_o·PO_4 parallel the rate of loss of activity.[18] Rate constants listed in Table 4 give an average value of 6.5(2) $\times 10^{-5}$ s^{-1}. Under anaerobic conditions no absorbance changes are observed over 6 h. The change in absorbance (ΔA) at the wavelength monitored (usually 620 nm) is dependent on the concentration of $H_2PO_4^-$, and for a given time interval was approximately twice as large with 100 as with 10 mM phosphate. Protein PAP_r without bound phosphate requires more than a week to convert into PAP_o. Reactions carried out with pyrophosphate and tripolyphosphate at 15 and 23 mM respectively gave similar first-order rate constants of 6.5×10^{-5} and 7.2×10^{-5} s^{-1} for the formation of PAP_o·PO_4. As will be reported elsewhere, $[Cr(CN)_6]^{3-}$ inhibits the oxidation of PAP_r by $[Fe(CN)_6]^{3-}$. Here $[Cr(CN)_6]^{3-}$ (2.1 mM) was found to have no effect on the oxidation of PAP_r (0.025 mM) by O_2 in the presence of $H_2PO_4^-$ (64 mM).

Reactivity of High M_r PAP_r.—At pH 5.0 no absorbance changes were observed at 508 nm for the reaction of $H_2PO_4^-$ (29–125 mM) with the high M_r heterodimer (4.0×10^{-5} M), in agreement with studies of Baumbach *et al.*[47] at pH 4.9 and 8.2. At lower pH the dimer slowly dissociates.[47] It was also noted that the dimer is much less susceptible to oxidation than is normal PAP_r.

Discussion

Although reactions of PAP_r with oxy-anions are well documented there has so far been no clear understanding of the mechanism of reaction, and the precise function of the Fe^{II} and Fe^{III} combination. While as yet no crystal structure is available, some general features of the active-site structure, Fig. 1, have been established from an extensive use of physical techniques. In the present work we have explored the reaction of in all nine different phosphates with PAP_r. Rate constants k_{obs} in five cases studied, Fig. 3, were found to be independent of $[PO_4]$ over the range 10–50 mM. The reactions with $H_2PO_4^-$ and phenyl phosphate were shown to be independent of acetate buffer (25–55 mM), and there is no evidence for extensive acetate complexing to either of the iron atoms. Significantly, in the case of $OP(OMe)_3$, no absorbance changes were observed over reaction times much in excess of those used for the other phosphates, indicating the contrasting behaviour of P=O and $P-O^-$, and the need for two strongly nucleophilic oxo groups (and/or more hydrophilic groups) for attachment to the iron(III) chromophore to occur. The inhibiting effect which $OP(OMe)_3$ has on the reaction with $H_2PO_4^-$ strongly suggests competitive

Table 4 The air oxidation (25 °C) of the PAP_r·PO_4 (uteroferrin) product to PAP_o·PO_4 at pH 5.0 (except as stated), I = 0.100 M (NaCl)

$[H_2PO_4^-]$/mM	9.0	17.0	17.0	24.0	45	89
$10^5 k_{obs}/s^{-1}$	6.8	7.1	6.6[a]	6.8	7.0	6.7
$[H_2PO_4^-]$/mM	89	103	119			
$10^5 k_{obs}/s^{-1}$	6.5[b]	6.9	6.5			

Pyrophosphate at 15 mM gave k_{obs} = 6.5(2) × 10^{-5} s^{-1}.
Tripolyphosphate at 23 mM gave k_{obs} = 7.2(3) × 10^{-5} s^{-1}.
[a] pH 3.5. [b] pH 6.0.

binding to an active region on the enzyme which might of course be the Fe^{II}. While association of substrate with the enzyme prior to attachment to an Fe may be important, and have to be included in a complete mechanism, we have no evidence as yet for its inclusion. On the other hand participation of Fe^{II} is required since on completion μ-PO_4 is present, and we proceed therefore on the assumption that Fe^{II} at least is involved in the early stages of reaction.

The various observations made provide support for phosphate binding first to the Fe^{II} in a relatively rapid process which does not contribute appreciably to the visible absorbance spectrum. Bridging to the strongly chromophoric Fe^{III} then occurs in a $[PO_4]$-independent step. The amplitude of the absorbance changes is dependent on $[PO_4]$, and the overall reaction (6) takes place therefore in two stages (7) and (8). In

$$Fe^{II}Fe^{III} + PO_4 \overset{K}{\rightleftharpoons} Fe^{II}\text{–}PO_4\text{–}Fe^{III} \quad (6)$$

$$Fe^{II}Fe^{III} + PO_4 \underset{k_{-x}}{\overset{k_x}{\rightleftharpoons}} PO_4\text{–}Fe^{II}Fe^{III} \quad (7)$$

$$PO_4\text{–}Fe^{II}Fe^{III} \underset{k_{-y}}{\overset{k_y}{\rightleftharpoons}} Fe^{II}\text{–}PO_4\text{–}Fe^{III} \quad (8)$$

these equations PO_4–$Fe^{II}Fe^{III}$ and Fe^{II}–PO_4–Fe^{III} are the monodentate Fe^{II}-co-ordinated phosphato and the bridging phosphato forms respectively. Rate constants k_{obs} for the bridge-closure equilibration process can be expressed as in equation (9). The fraction of protein present as PO_4–Fe^{II}–Fe^{III}

$$k_{obs} = k_y + k_{-y} \quad (9)$$

is retained at a constant level by the fast equilibration (7). While we have determined the overall K we have no information regarding K_x for (7), except that the interpretation requires $K_x[PO_4] \gg 1$. Either K_x is bigger than expected therefore (assistance from an amino acid?), or a further elaboration of the mechanism is required.

Rate constants k_{obs} are dependent on pH, Figs. 4 and 5. The mechanism of the reaction with $H_2PO_4^-$ is considered first. The pK_a values of H_3PO_4 (2.12) and $H_2PO_4^-$ (6.7) are consistent with $H_2PO_4^-$ as the dominant reactant species in the present studies. The decrease in k_{obs} with pH, Fig. 4, gives a pK_a of 3.9 (not particularly well defined at the lower pH) suggesting involvement of an iron(III)-bound H_2O. For comparison the first acid dissociation constant for $[Fe(H_2O)_6]^{3+}$ is 3.0, whereas $[Fe(H_2O)_6]^{2+}$ remains in the aqua form until pH ≥7.[48] The behaviour observed therefore is consistent with participation of aqua and hydroxo (conjugate-base) forms of the Fe^{III}. At between pH 3 and 4 other acid dissociation processes on the enzyme may contribute again suggesting that this pK_a should be regarded as very approximate.

A common feature of biological reactions involving substrate to metal binding is the ability of the metal to change its co-ordination number rather than be involved in a more lengthy ligand-substitution process, *e.g.* zinc(II) enzymes,[49] and O_2-binding proteins such as haemerythrin.[50] In the present case the Fe^{II} may well be five-co-ordinate as in the case of the binuclear iron(II) protein deoxyhaemerythrin.[50] Although there are unusual examples of Fe^{III} adopting seven-co-ordinate structures,[46] the iron(III) situation requires more extensive discussion (see next paragraph). Alternatively a bridge-cleavage process or change involving chelated to monodentate carboxylate at the Fe^{III} (as observed in the reduction of the binuclear iron enzyme ribonucleotide reductase[51]) would be ways of providing a co-ordination vacancy. If substitution is involved then the properties of Fe^{II} and Fe^{III} are indicated in a very general way by reference to the aqua ions. Thus it is known that high-spin $[Fe(H_2O)_6]^{2+}$ has a water-exchange rate constant of *ca.* 10^6 s^{-1} which is 10^2–10^3 times greater than the value for high-spin $[Fe(H_2O)_6]^{3+}$.[52,53] Whichever mechanism is relevant, rapid binding of phosphate to the Fe^{II} is a perfectly reasonable first stage. This is followed by the slower bridge-forming attachment of the phosphate to the Fe^{III} in a $[PO_4]$-independent step. Phosphate bridge closure has been studied previously in the reaction of the binuclear cobalt(III) complex $[(NH_3)_4Co(\mu\text{-}NH_2)(\mu\text{-}OH)Co(NH_3)_4]^{4+}$ with $H_2PO_4^-$,[54] which is a somewhat different process since both the Co^{III} atoms are chromophoric and have identical substitution properties.

In studies on the reaction of PAP_r with α-naphthyl phosphate it is possible to follow the release of α-naphthol which has a prominent peak at 323 nm, as a means of monitoring the phosphate (hydrolysis) activity, Fig. 7. Determination of k_{obs} was not possible as with other reactants because of the limited solubility of the α-naphthol. Maximum activity is observed at pH 4.9. Similarly with *p*-nitrophenyl phosphate maximum activity has been observed at 4.9.[55] This corresponds to the pH at which the first acid dissociation giving Fe^{III}–OH could well peak. We note that in the case of *p*-nitrophenyl phosphate the k_{obs} values (from absorbance changes at 620 nm) decrease with increasing pH (3.18 to 3.89), and are numerically very similar to those for phenyl phosphate, Fig. 4.

From these observations it can be concluded that Fe^{III}–OH, or a related conjugate-base form, induces phosphate hydrolysis. Rate constant k_{obs} are however at a maximum at pH ≈3 when Fe^{III}–H_2O is present, Figs. 4 and 5. Therefore bridge closure making use of a co-ordination change at the Fe^{III}, or with displacement of the H_2O, gives little or no hydrolysis, (10). At higher pH the hydroxo ligand of Fe^{III}–OH substitutes into the phosphorus(v) co-ordination sphere with (in the general case) displacement of RO^- from $O_3P(OR)^{2-}$, equation (11). The

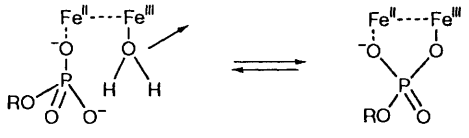

(10)

(11)

reaction sequence proposed has a number of features in common with the intramolecular phosphate hydrolysis occurring in the case of $[Co(en)_2(H_2O)\{PO_3(OC_6H_4NO_2)\}]^+$ (en = ethylenediamine), and involving the conjugate-base $[Co(en)_2(OH)\{PO_3(OC_6H_4NO_2)\}]$.[56]

The mechanism that emerges from the present studies in one of repeated bridge formation and cleavage, with hydrolysis taking place on a subsequent if not the first cycle. The full mechanism is shown in Scheme 1, with $H_2PO_4^-$ as reactant. The shapes of this and other pH profiles, Figs. 4 and 5, indicate different degrees of acid dissociation of the phosphato iron(II) co-ordinated intermediates and pK_{2a} (and k_3) involvement. Table 2 summarises the data obtained. A list of literature pK_a values for the different uncomplexed phosphate species is given in Table 3. Some shifts in pK_a are observed as a result

of complexing of the phosphate to the Fe^{II}, and corresponding trends in rate constants are observed.[54] In the case of $H_2PO_4^-$ it would appear that the pK_a of 6.7 is not shifted sufficiently on attachment of Fe^{II} for this pK_a to become relevant. A pK_{2a} step is observed with phenyl phosphate, but the effect is relatively small, Fig. 4. With pyrophosphate and tripolyphosphate the pK_{2a} values are more clearly defined and in the range 5.0–5.3, with pK_a shifts of 0.3–0.5 as compared to the free phosphates.

The reaction of the $[Co(NH_3)_5(HPO_4)]^+$ complex with PAP_r is observed to be strictly uniphasic and appreciably faster than aquation of the phosphate.[40] The steric bulkiness and/or charge on the complex appears drastically to inhibit PAP_r catalysis of the aquation/hydrolysis process.

The activity of PAP_r and extent of hydrolysis occurring decreases at pH > 4.9, Fig. 7. We have not studied this range of pH in any detail. Contributing factors might include deprotonation of the substrate, acid dissociation of an H_2O attached to the Fe^{II}, or polypeptide acid dissociation process(es).

Rate constants k_{obs} at pH 4.6, Fig. 3, are in the range 1.03–2.24 s^{-1}, and exhibit little change with type of phosphate involved. Values of k_1/s^{-1} are for phosphate (7.1), phenyl phosphate (8.4), pyrophosphate (4.7), tripolyphosphate (3.1) and ATP ($\approx$3.8), consistent with at most a small dependence on size. As far as the charge on the various reactants is concerned, these are present at *e.g.* pH $\approx$3.5 as $H_2PO_4^-$, $(PhO)HPO_3^-$, $H_2P_2O_7^{2-}$, $H_2P_3O_{10}^{3-}$ and ATP (2−), and there is no obvious dependence on the magnitude of the negative charge. As previously mentioned the possibility that there is association/ion pairing of the reactants to PAP_r prior to attachment to the Fe^{II} cannot be ruled out. The protein has a $pI > 9.6$, and at pH ≤ 7 will retain a substantial positive charge.[57] From known formation constants for Fe^{II} and Fe^{III} with phosphate, Fe^{III} would be expected to have at least an order of magnitude greater affinity for phosphate than does Fe^{II}.[58,59] Initial association with Fe^{III} might be expected if the Fe^{III} were five-co-ordinate as in Fig. 1. However the $[PO_4]$-independent rate law argues against this.

The first-order kinetic plots for k_{obs} exhibit no further dependences which can be attributed to the need for recycling as the reactants $O_3P(OR)^{2-}$ are hydrolysed. Thus in equation (9) the rate constant k_{-y} appears to be invariant as the reactions proceed. The absorbance changes are small however, Fig. 2, and in view of the similarity of the reagents used this should not be regarded as evidence against the mechanism proposed. Since experimentally determined rate constants lie well within an order of magnitude of each other, it is unlikely that k_y and k_{-y} vary much as the identity of the phosphate reactant changes. As far as the possibility of a bridge-closure substitution step k_y is concerned, a dissociative S_N1 process in which Fe^{III}–H_2O bond breaking is rate determining might be considered. However rate constants fall far short of the water-exchange rate constant for substitution on $[Fe(H_2O)_6]^{3+}$, and effects from other iron(III) ligands and/or adjacent residues would have to be influential. For a fuller consideration of equilibration kinetic situations, some of which are relevant in the present case, the reader is referred to studies on the chelation of bipyridine to $[Cr(H_2O)_6]^{2+}$.[60]

Previously[32] it has been reported that the reduction potential for the PAP_o–PAP_r couple of 367 mV at pH 5.0 decreases to 183 mV on phosphate binding, increasing the susceptibility of the protein to air oxidation. From present studies rate constants for the phosphate-induced oxidation using air-saturated solutions remain small, and are independent of $[H_2PO_4^-]$ (9–119 mM) and pH (3.5–6.0). Amounts of the phosphato-bridged $Fe^{II}Fe^{III}$ reactant are replenished in the fast equilibration prior to oxidation by O_2. As a result complete conversion into $Fe^{III}Fe^{III}$ is observed. We have no information as to the mechanism and whether this involves an inner- or outer-sphere oxidation by O_2. Thus the reactive form of the protein has phosphate co-ordinated to both metal centres,[30] and there is no evidence for other co-ordinated H_2O groups. This is substantiated in the case of the Fe^{III} by rate constants exhibiting no dependence on pH.

The ability of zinc(II) to replace iron(II) in plant PAP and initiate similar chemistry is of considerable interest.[14] Thus zinc(II) is known to exhibit different co-ordination numbers from four to six, and is more labile than is Fe^{II}.[52] These properties support such a functional role, without the added complication of redox changes as in the case of Fe^{II}.

Finally as far as phosphate ester hydrolysis is concerned, we note that steps involving Fe^{III}–OH, k_2 and k_3 in Table 2, are many orders of magnitude faster than the uncatalysed hydrolysis,[61] but on a biological time-scale are quite slow. Whether the specificity of the protein for certain ester groups might lead to more favourable interactions is of further interest.

Acknowledgements

We thank the SERC (J.-S. L.) and NATO/Natural Sciences and Engineering Research Council of Canada (MASA) for post-doctoral support.

References

1 J. B. Vincent, G. L. Olivier-Lilley and B. A. Averill, *Chem. Rev.*, 1990, **90**, 1447.
2 B. C. Antanaitis and P. Aisen, *J. Biol. Chem.*, 1984, **259**, 2066.
3 W. C. Buhi, F. W. Bazer, C. Ducsay, P. W. Chun and R. M. Roberts, *Fed. Proc., Fed. Am. Soc. Exp. Biol.*, 1979, **38**, 733.
4 J. C. Davis and B. A. Averill, *Proc. Natl. Acad. Sci. USA*, 1982, **79**, 4623.
5 B. C. Antanaitis and P. Aisen, *J. Biol. Chem.*, 1982, **257**, 1855.
6 D. F. Hunt, J. R. Yates III, J. Shabonowitz, N.-Z. Zhu, T. Zirino, B. A. Averill, S. T. Daurat-Larroque, J. G. Shewale, R. M. Roberts and K. Brew, *Biochem. Biophys. Res. Commun.*, 1987, **144**, 1154.
7 P. R. Nuttleman and R. M. Roberts, *J. Biol. Chem.*, 1990, **265**, 12192.
8 C. M. Ketcham, R. M. Roberts, R. C. M. Simen and H. S. Nicke, *J. Biol. Chem.*, 1989, **264**, 557.
9 P. G. Debrunner, M. P. Hendrich, J. de Jersey, D. T. Keough, J. T. Sage and B. Zerner, *Biochim. Biophys. Acta*, 1983, **745**, 103.
10 K. Cichutek, H. Witzel and F. Parak, *Hyperfine Interactions*, 1988, **42**, 885.
11 B. C. Antanaitis, P. Aisen and N. R. Lilienthal, *J. Biol. Chem.*, 1983, **258**, 3166.
12 B. P. Gaber, J. P. Sheridan, F. W. Bazer and R. M. Roberts, *J. Biol. Chem.*, 1979, **254**, 8340.
13 B. A. Averill, J. C. Davis, S. Burmann, T. Zirino, J. Sanders-Loehr, T. M. Loehr, J. T. Sage and P. G. Debrunner, *J. Am. Chem. Soc.*, 1987, **109**, 3760.
14 J. L. Beck, L. A. McConachie, A. C. Summers, W. N. Arnold, J. de Jersey and B. Zerner, *Biochim. Biophys. Acta*, 1986, **869**, 61.
15 S. K. Heffer and B. A. Averill, *Biochem. Biophys. Res. Commun.*, 1987, 1173.
16 S. Fujinoto, A. Ohara and K. Uehara, *Agric. Biol. Chem.*, 1980, **44**, 1659.
17 B. Krebs, M. Körner, H. Suerbaum and H. Witzel, *J. Mol. Biol.*, 1992, **224**, 511.
18 J. W. Pyrz, J. T. Sage, D. G. Debrunner and L. Que, jun., *J. Biol. Chem.*, 1986, **261**, 11015.
19 R. G. Wilkins, *Chem. Soc. Rev.*, 1992, **21**, 171.
20 J. L. Beck, D. T. Keough, J. de Jersey and B. Zerner, *Biochim. Biophys. Acta*, 1984, **791**, 357.
21 S. M. Kauzlarich, B. K. Teo, S. Burmann, J. C. Davis and B. A. Averill, *Inorg. Chem.*, 1986, **25**, 2781.
22 Z. Wang, L.-J. Ming, L. Que, jun., J. B. Vincent, M. W. Crowder and B. A. Averill, *Biochemistry*, 1992, **31**, 5263.
23 R. C. Holz, L. Que, jun., and L.-J. Ming, *J. Am. Chem. Soc.*, 1992, **119**, 4434.
24 R. B. Lauffer, B. C. Antanaitis, P. Aisen and L. Que, jun., *J. Biol. Chem.*, 1983, **258**, 14212.
25 R. C. Scarrow, J. W. Pyrz and L. Que, jun., *J. Am. Chem. Soc.*, 1990, **112**, 657.
26 B. C. Antanaitis, J. Peisach, W. B. Mims and P. Aisen, *J. Biol. Chem.*, 1985, **260**, 4572.
27 M. W. Crowder, J. B. Vincent and B. A. Averill, *Biochemistry*, 1992, **31**, 9603.
28 J. L. Beck, L. A. McConachie, A. C. Summers, W. N. Arnold, J. de Jersey and B. Zerner, *Biochim. Biophys. Acta*, 1986, **869**, 61.

29 E. P. Day, S. S. David, J. Peterson, W. R. Dunham, J. J. Bonvoisin, R. M. Sands and L. Que, jun., *J. Biol. Chem.*, 1988, **263**, 15561.
30 A. E. True, R. C. Scarrow, C. R. Randell, R. C. Holz and L. Que, jun., *J. Am. Chem. Soc.*, 1993, **115**, 4246.
31 K. Doi, J. McCracken, J. Peisach and P. Aisen, *J. Biol. Chem.*, 1988, **263**, 5757.
32 D. L. Wang, R. C. Holz, S. S. David, L. Que, jun., and M. T. Stankovich, *Biochemistry*, 1991, **30**, 8187.
33 E. G. Mueller, M. W. Crowder, B. A. Averill and J. R. Knowles, *J. Am. Chem. Soc.*, 1993, **115**, 2974.
34 M. Dietrich, D. Münstermann, H. Suerbaum and H. Witzel, *Eur. J. Biochem.*, 1991, **199**, 105.
35 J. B. Vincent, M. W. Crowder and B. A. Averill, *Biochemistry*, 1992, **31**, 3033; *J. Biol. Chem.*, 1991, **266**, 17737; *Biochemistry*, 1991, **30**, 3025.
36 D. C. Crans, C. M. Simone, R. C. Holz and L. Que, jun., *Biochemistry*, 1992, **31**, 11731; *J. Biol. Chem.*, 1991, **266**, 11737.
37 S. S. David and J. Que, jun., *J. Am. Chem. Soc.*, 1990, **112**, 6455.
38 M. A. S. Aquino, J.-S. Lim and A. G. Sykes, *J. Chem. Soc., Dalton Trans.*, 1992, 2135.
39 J. C. Davis, S. S. Lin and B. A. Averill, *Biochemistry*, 1981, **20**, 4062.
40 (*a*) W. Schmidt and H. Taube, *Inorg. Chem.*, 1963, **2**, 698; (*b*) S. F. Lincoln and D. R. Stranks, *Aust. J. Chem.*, 1968, **21**, 37.
41 OLIS, Bogart, GA.
42 H. Sigel, K. Becker and D. B. McCormick, *Biochim. Biophys. Acta*, 1967, **148**, 655.
43 E. J. King and G. E. Delory, *Biochem. J.*, 1939, **33**, 1185.
44 A. Johansson and E. Wänninen, *Talanta*, 1963, **10**, 769.
45 G. Weitzel and T. Speer, *Hopper Seyer's Z. Physiol. Chem.*, 1958, **313**, 212; Y. Handschin and H. Brintzinger, *Helv. Chim. Acta*, 1962, **99**, 383; P. W. Schneider, H. Brintzinger and H. Erlenmeyer, *Helv. Chim. Acta*, 1964, **47**, 992.
46 M. D. Lind, M. J. Hamor, T. A. Hamor and J. L. Hoard, *Inorg. Chem.*, 1964, **3**, 34.
47 G. A. Baumbach, C. M. Ketcham, D. E. Richardson, F. W. Bazer and R. M. Roberts, *J. Biol. Chem.*, 1986, **261**, 12869.
48 C. F. Baes and E. Mesmer, *The Hydrolysis of Cations*, Wiley-Interscience, New York, 1976.
49 B. L. Vallee and D. S. Auld, *Biochemistry*, 1990, **29**, 5647.
50 R. E. Stenkamp, L. C. Sieker, L. H. Jensen, J. D. McCallum and J. Sanders-Loehr, *Proc. Natl. Acad. Sci. USA*, 1985, **82**, 713.
51 P. Nordlund, B.-M. Sjöberg and H. Eklund, *Nature (London)*, 1990, **354**, 593; P. Nordlund, A. Åberg, H. Eklund, K. Regnstran and J. Hajdu, in the press.
52 See, for example, R. G. Wilkins in *Kinetics and Mechanism of Reactions of Transition Metal Complexes*, VCH, Weinheim, 1991.
53 T. W. Swaddle and A. E. Merbach, *Inorg. Chem.*, 1981, **20**, 4212.
54 J. D. Edwards, S. W. Foong and A. G. Sykes, *J. Chem. Soc., Dalton Trans.*, 1973, 829.
55 D. C. Schlosnagle, F. W. Bazer, J. C. M. Tsibris and R. M. Roberts, *J. Biol. Chem.*, 1974, **249**, 7574.
56 P. Hendry and A. M. Sargeson, *Prog. Inorg. Chem.*, 1990, **38**, 201.
57 B. C. Antanaitis and P. Aisen, *Adv. Inorg. Biochem.*, 1983, **5**, 111.
58 J. O. Nriago, *Geochim. Cosmochim. Acta*, 1972, **36**, 459.
59 S. Ramamoorthy and D. G. Manning, *Inorg. Nucl. Chem. Lett.*, 1973, **10**, 109.
60 H. Diebler, *Ber. Bunsenges. Phys. Chem.*, 1970, **74**, 268.
61 See, J. E. Coleman and P. Gettins, in *Zinc Enzymes*, ed. T. Spiro, Wiley, New York, 1983, p. 153.

Received 30*th June* 1993; *Paper* 3/03757F